Int J Thermophys (2012) 33:640–652
DOI 10.1007/s10765-011-1061-4

Effect of the Molecular Weight of Poly(ethylene glycol) on the Properties of Biocompatible Magnetic Fluids

A. Józefczak · T. Hornowski · A. Skumiel · V. Závišová · M. Koneracká · N. Tomašovičová · M. Timko · P. Kopčanský · H. N. Kelani

Received: 1 April 2011 / Accepted: 26 July 2011 / Published online: 13 August 2011
© The Author(s) 2011. This article is published with open access at Springerlink.com

Abstract The effect of the molecular weight of poly(ethylene glycol) (PEG) on the physical properties of water-based magnetic fluids with sodium oleate and PEG stabilization was investigated. The structure as well as magnetic, rheological, and thermal properties of the obtained samples were studied using transmission electron microscopy (TEM), photon cross correlation spectroscopy (PCCS), superconducting quantum interference device (SQUID), and differential scanning calorimetry (DSC) methods. The molecular weight of PEG had a strong effect on the rheological properties while the effect was rather insignificant on the particle size distribution and the self-heating of the studied magnetic fluids. The heating ability of the PEG-stabilized magnetic fluids was determined by calorimetric measurements of the specific absorption rate (SAR). The thickness of the PEG layer was calculated from the experimental data of the temperature rise rates as a function of the magnetic field strength using the Rosensweig theory.

Keywords Hyperthermic effect · Magnetic fluid · Nanoparticles · PEG

1 Introduction

Superparamagnetic iron oxide nanoparticles have been widely used for medical applications. Especially, *in vivo* applications of nanoparticles require highly biocompatible

A. Józefczak (✉) · T. Hornowski · A. Skumiel · H. N. Kelani
Institute of Acoustics, Faculty of Physics, Adam Mickiewicz University, Umultowska 85, 61-614 Poznań, Poland
e-mail: aras@amu.edu.pl

V. Závišová · M. Koneracká · N. Tomašovičová · M. Timko · P. Kopčanský
Institute of Experimental Physics, Slovak Academy of Sciences, Watsonova 47, 040 01 Košice, Slovakia

particle surfaces. Coatings can improve oxidation resistance, the ability to functionalize, phagocyte resistance, mechanical stability, and biocompatibility. Many synthetic and natural polymers such as dextran, polyethylene glycol (PEG), or polyethylene oxide (PEO) are biocompatible and may be used as coatings. Poly(ethylene glycol) is a linear polymer consisting of repeated units of CH_2-CH_2-O, the number of which depends on the molecular weight. Polyethylene glycol and related polymers covalently bond to surfaces or are adsorbed on magnetic nanoparticles and can prolong the circulation time in the bloodstream [1,2]. The immobilization of PEG on nanoparticles increases the amount of nanoparticle uptake into cancer cells in comparison to unmodified nanoparticles [3]. These particles have found applications in magnetic drug targeting [4,5] and magnetic hyperthermia [6,7]. The PEG-coated nanoparticles could be used also as safe MR contrast agents [2,5].

The delivery of nanoparticles in the human body usually requires suspending the nanoparticles in a water-based fluid, forming a homogeneous suspension, called a ferrofluid. Magnetic nanoparticles must remain suspended in the fluid and cannot form aggregates due to van der Waals or magnetic interactions [1].

In this study, we investigated the effect of the addition of PEG as a surface modifier on the physical properties of nanoparticle suspensions, especially the effect of the molecular weight of PEG on the physical properties of water-based magnetite ferrofluids.

2 Sample Preparation

Poly(ethylene glycol) with average molecular weights of 400, 1000, 10 000, and 20 000 were provided by Sigma-Aldrich. Sodium oleate was obtained from Riedel-de Haën. Typically, ferric chloride hexahydrate ($FeCl_3 \cdot 6H_2O$), ferrous sulfate heptahydrate ($FeSO_4 \cdot 7H_2O$), and ammonium hydroxide (NH_4OH) were used for magnetite synthesis. The co-precipitation method of ferric and ferrous salts in an alkaline aqueous medium was used to prepare spherical magnetite particles. In a typical synthesis, an aqueous solution of Fe^{3+} and Fe^{2+} in a molar ratio 2:1 was prepared by dissolving in deionized water. To the mixture of Fe^{3+} and Fe^{2+} ions, an excess of hydroxide ions was added at room temperature with vigorous stirring. A black precipitate of magnetite nanoparticles was immediately formed. After washing the precipitate by magnetic decantation and heating to 50 °C, the surfactant sodium oleate ($C_{17}H_{33}COONa$) was added to the mixture to prevent agglomeration of the particles. This mixture was stirred with heating until the boiling point was reached. Magnetite particles stabilized by an oleate bilayer were dispersed in water. Agglomerates were removed by centrifugation (9000 rpm for 30 min). Finally, PEG was used to improve the biocompatibility of the prepared magnetic fluid. PEG with molecular weights of 0.4, 1, 10, and 20 kDa, dissolved in water, was added to the initial magnetic fluid at 50 °C. The mixture was stirred for half an hour. A magnetic fluid—magnetite particles coated with sodium oleate and PEG—was formed in this way [8]. Infrared spectroscopy and digital scanning calorimetry measurements showed that after such a procedure, PEG adsorbs on the magnetite [8,9]. All samples contained the same amount of PEG—20.69 mg per mL of magnetic fluid. The magnetic fluid (denoted as MK) with only an oleate

surfactant layer was also studied for comparison. The appropriate amount of distilled water was added to this sample to obtain the same concentration of magnetic material.

3 Measurements, Results, and Discussion

Obtained samples were tested using the following experimental methods of measurement: superconducting quantum interference device (SQUID), differential scanning calorimetry (DSC), transmission electron microscopy (TEM), photon cross correlation spectroscopy (PCCS), and calorimetric measurements (CM). Also, the density and viscosity of the samples were measured.

3.1 Magnetic Properties

Magnetic measurements of the samples were carried out with the aid of a SQUID. A SQUID magnetometer was used to measure the magnetization curves from which the volume concentration of the magnetite particles in magnetic liquids, the average diameter of magnetite particles, and the particle size distribution function (PSD) were determined. The magnetization curves for MK400 and MK20 000 samples measured at room temperature are shown in Fig. 1a. The magnetic measurements in all samples confirmed the superparamagnetic behavior of the nanoparticles with no hysteresis. Figure 1b shows a magnetic core of the Fe_3O_4 particle size distribution function $F(x)$ extracted from magnetic measurements with the assumption that the magnetization is the superposition of Langevin functions, $L(\xi) = \coth\xi - 1/\xi$ [10],

$$M = M_s \int_0^\infty L(\xi) F(x) \mathrm{d}x, \tag{1}$$

where $\xi = \mu_0 M_d H V_m / (k_B T)$, μ_0 is the permeability of free space, k_B is the Boltzmann constant, V_m is the volume of magnetic core, and $M_d = 334\,\mathrm{kA} \cdot \mathrm{m}^{-1}$ (for magnetite) is the bulk magnetization of the suspended particles. $M_s = \phi M_d$ is the saturation magnetization, and ϕ is the volume concentration of magnetic particles. A good fit of Eq. 1 to the measured magnetization data can be obtained using the log-normal distribution as the particle size distribution function,

$$F(x) = \frac{1}{\sqrt{2\pi}Sx} \exp\left[\frac{-(\ln x/D)^2}{2S^2}\right]. \tag{2}$$

From the parameters of the distribution, D and S, the mean diameter $\langle x \rangle$ and standard deviation of the particle size, σ, can be calculated.

The values of the magnetic parameters obtained for all studied samples are listed in Table 1.

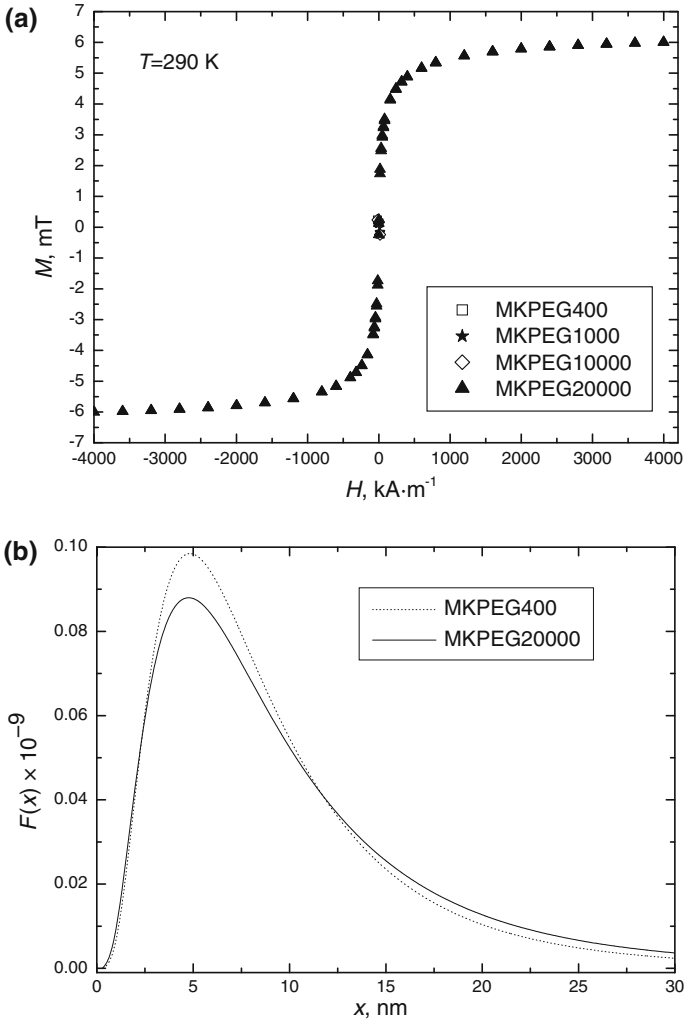

Fig. 1 (a) Hysteresis loops $M(H)$ for the MKPEG400 and MKPEG20 000 samples obtained from SQUID data and (b) particle magnetic core size distributions calculated from Eq. 1

Table 1 Concentration of magnetic material, ϕ_m, concentration of PEG stabilizer, ϕ_{PEG}, saturation magnetization, M_S, parameters, D, S, of magnetic core size distribution, mean diameter of magnetic core, $\langle x \rangle$, and standard deviation of magnetic core size, σ, for studied samples

Samples	ϕ_m ($g \cdot L^{-1}$)	ϕ_{PEG} ($g \cdot L^{-1}$)	M_S (mT)	D (nm)	S	$\langle x \rangle$ (nm)	σ (nm)
MKPEG 400	80.31	20.69	6.52768	8.06	0.731	10.53	8.85
MKPEG 1000	79.50	20.69	6.46687	7.56	0,672	9.47	7.16
MKPEG 10 000	78.78	20.69	6.41933	8.10	0.734	10.57	8.87
MKPEG 20 000	78.66	20.69	6.39392	8.15	0.712	10.49	8.49

3.2 Structure and Morphology of Magnetic Nanoparticles

The prepared samples were observed by transmission electron microscopy (TEM) to obtain information about morphology and surface characterization of the nanoparticles. Figure 2 shows the TEM micrograph of magnetite/sodium oleate/PEG composite nanoparticles. The TEM image showed that nanoparticles were nearly

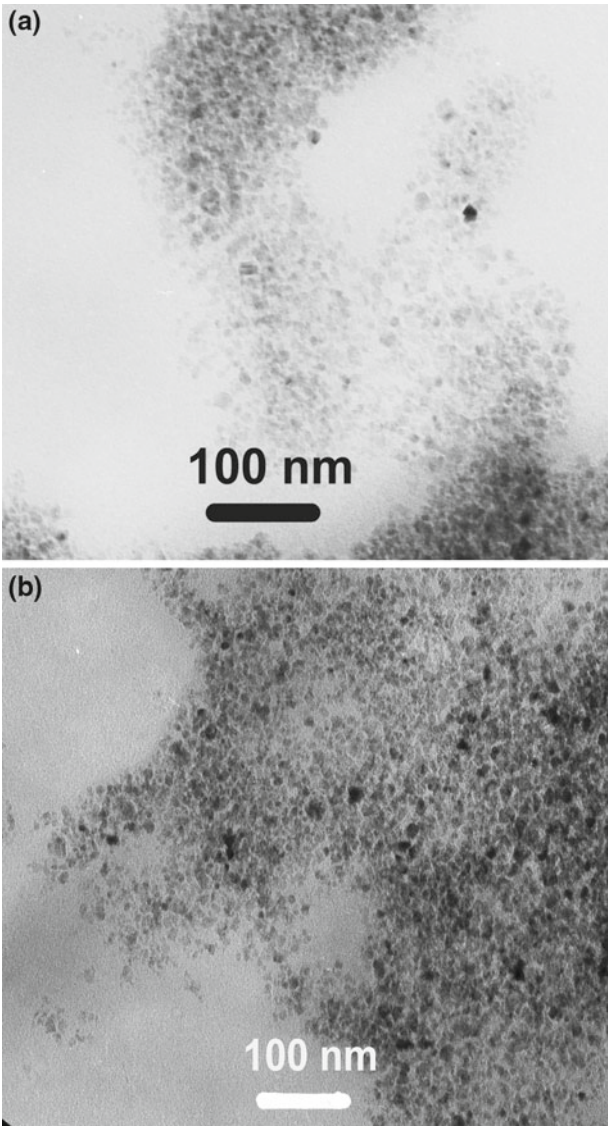

Fig. 2 TEM images of (a) MKPEG10 000 and (b) MKPEG20 000

spherical in shape and polydisperse with an average size of the magnetic core of about 10 nm.

3.3 Photon Cross Correlation Spectroscopy

After coating, the particle size increases. The diameter, d_h, of the nanoparticle with surfactant layer or layers is called the "hydrodynamic diameter." It is greater than the size of the magnetic core by a magnitude $\delta = 2(\delta_o + \delta_p)$ where δ_o denotes the thickness of the first surfactant protective layer (sodium oleate) and δ_p is the thickness of second surfactant layer—the PEG shell.

The mean hydrodynamic diameter of the poly(ethylene) glycol-coated magnetic nanoparticle depends on the concentration and molecular weight of the PEG polymer used for coating. The increase of δ_p with increasing concentration of PEG is considered as the result of the increased amount of adsorbed polymer. This leads to the development of polymer coils that form thicker and more compact adsorption layers on the surface of nanoparticles. The increase of the molecular weight of PEG favors a rich structure with loop and tail conformations during PEG adsorption [11]. Daou et al. [12] have shown that the average size of the coated nanocrystals increases with the increase of the PEG molecular weight in a linear fashion up to 12 000 Da, before reaching a plateau for 22 000 Da. On the other hand, Ren et al. [13] have shown that with the increase of the PEG molecular weight, the hydrophilicity of a synthesized copolymer enhances, which leads to a smaller interfacial tension between the polymer solution and water and gives rise to a smaller particle size.

The distribution of the hydrodynamic size of the magnetic nanoparticles was measured by PCCS. The results are shown in Fig. 3. The average size is larger than that found in the magnetic measurements. This is due to the fact that PCCS measurements are mostly determined by large particles that are present in the sample. The PCCS signal derived from nanoparticles with diameters far below the laser wavelength is dominated by Rayleigh scattering in which the intensity of the signal depends on the diameter of the particle, specifically the diameter raised to the power of six [14].

Figure 3 also shows that there is no distinct influence of the molecular weight of PEG on the hydrodynamic size of the magnetic nanoparticles. Probably, the PEG with a greater molecular weight gave a dense coating over the surface of the nanoparticles [2], and therefore, the length of the PEG chain became an insignificant factor in terms of the hydrodynamic size of nanoparticles.

3.4 Effect of PEG Coating on Density and Rheological Behavior of Magnetic Fluids

The density of magnetic fluids was measured using an oscillating U-tube density meter method. Figure 4 shows the experimental results for the density as a function of temperature. The density of the suspension decreases with increasing temperature. The density of the studied magnetic fluids depends on the PEG molecular weight. The

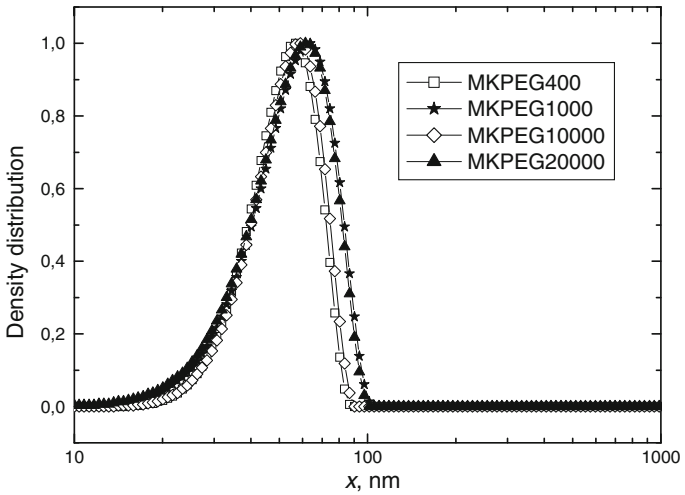

Fig. 3 Distributions of the hydrodynamic size of the magnetic nanoparticles measured using PCCS

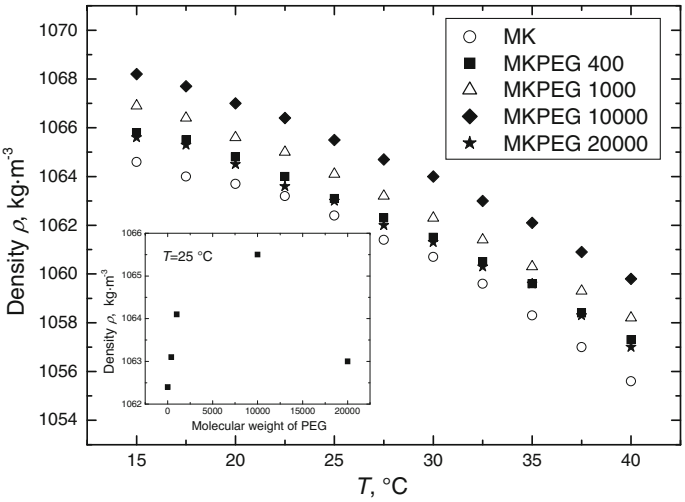

Fig. 4 Density dependence on temperature for the studied samples. *Inset* shows the density as a function of the molecular weight of PEG

density first increases with the PEG molecular weight, attains a maximum value for 10 000 Da, and then starts to decrease (Table 2).

The shear viscosity coefficient of the studied fluids was measured using a rotation rheometer in a cone-plate geometry. Figure 5 shows the shear stress versus shear rate flow curves. The linear flow curves were obtained for all samples. It means that in the absence of a magnetic field, the magnetic fluids studied in this experiment behaved as Newtonian fluids. This is in agreement with the finding that the magnetic fluids show typical Newtonian behavior when the solid content is low and exhibit strong

Table 2 Density and viscosity of a magnetic nanoparticle suspension in water before and after the PEG coating ($T = 30\,^{\circ}\mathrm{C}$)

Samples	Density ρ (kg · m^{-3})	Viscosity η (mPa · s)
MK	1060.7	1.516
MKPEG 400	1061.5	1.400
MKPEG 1000	1062.3	2.564
MKPEG 10000	1064.0	2.564
MKPEG 20000	1061.3	3.552

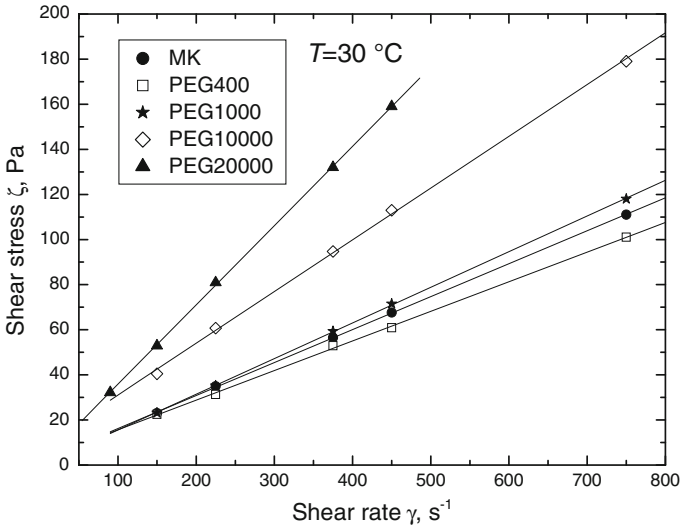

Fig. 5 Effect of the PEG molecular weight on shear stress versus shear rate flow curves

non-Newtonian behavior when the solid content is above $0.200\,\mathrm{g}\cdot\mathrm{mL}^{-1}$ [15,16]. The measured viscosity of the magnetic fluids before and after the addition of PEG is plotted against the temperature in Fig. 6. In the absence of the magnetic field, the viscosity increases with an increase of the PEG molecular weight and decreases with temperature according to the Arrhenius equation.

3.5 Hyperthermic Effect

The suitability of the PEG-stabilized magnetic fluids in hyperthermic therapy was determined by calorimetric measurements carried out in the experimental setup described earlier [17]. Figure 7 shows the rate of the temperature rise in the MKPEG20000 sample as indicated by $\Delta T/\Delta t$ at $t \approx 0$ for different values of the amplitude of an alternating magnetic field, H_0, and for the frequency, $f = 450\,\mathrm{kHz}$, of the field variations. An obvious heating effect can be observed. However, the rates of the temperature rise and the maximum temperatures attained were at moderate levels.

The self-heating of the magnetic fluids under the influence of the ac external magnetic field is a result of absorbing energy from the field and converting it into heat

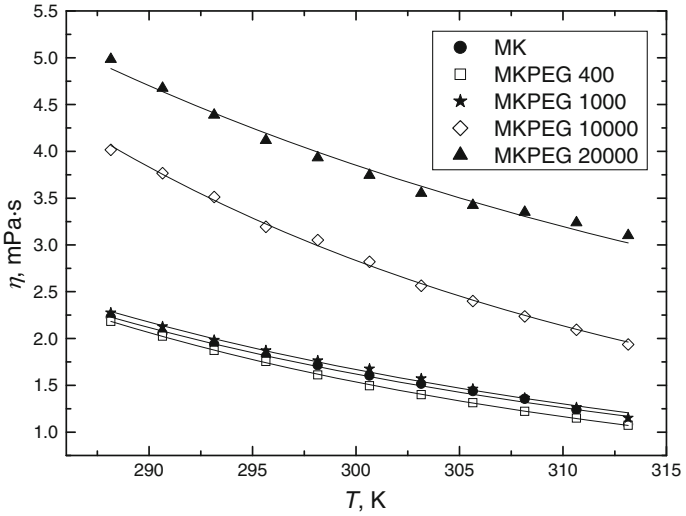

Fig. 6 Temperature dependence of the shear viscosity for the magnetic fluid samples. *Solid lines* represent the fits of the Arrhenius-type equation, $\eta = Ae^{B/(k_B T)}$, to the experimental data

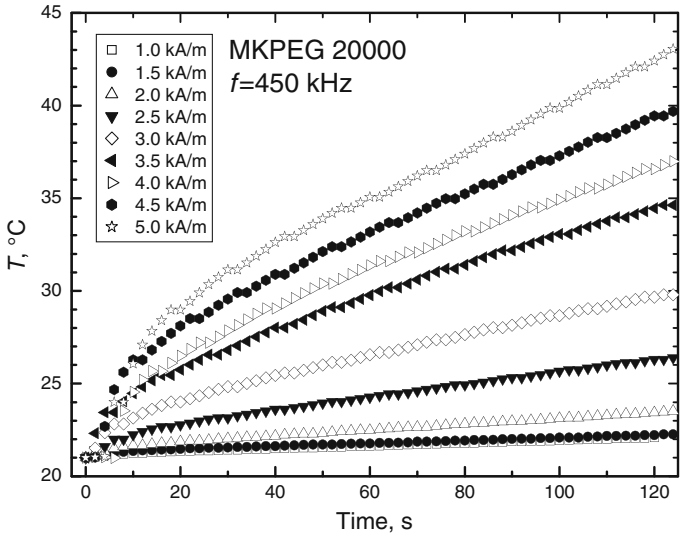

Fig. 7 Temperature versus time for the MKPEG20 000 sample for different values of the alternating magnetic field and for the frequency $f = 450$ kHz

by means of three mechanisms: eddy current losses, hysteresis losses during reversal of magnetization, and relaxation losses during the re-orientation of magnetization. The eddy current losses are negligible since a magnetic fluid has very low electrical conductivity. The samples tested showed no hysteresis (Fig. 1a), so there is no energy loss due to hysteresis. Thus, the only contribution to the magnetic field energy loss in the studied fluids comes from relaxation losses. For the polydispersive magnetic fluid

with a particle size (diameter) distribution $F(x)$, the heat dissipation due to relaxation losses can be expressed as [18]

$$P = \pi \mu_0 H_0^2 f \int_0^\infty \chi_i \frac{3}{\xi} \left(\coth \xi - \frac{1}{\xi} \right) \frac{2\pi f \tau}{1 + (2\pi f \tau)^2} F(x) \mathrm{d}x, \tag{3}$$

where $\chi_i = \mu_0 \phi M_\mathrm{d}^2 V_\mathrm{m} / (3 k_\mathrm{B} T)$ is the initial susceptibility. There are two mechanisms by which the magnetization of a magnetic fluid may relax after removing the applied magnetic field: the Brown and the Néel mechanisms. The Brown mechanism involves rotations of the entire nanoparticle relative to the surrounding medium, with its magnetic moment locked in an axis of easy magnetization. Its relaxation time is given by the following relationship:

$$\tau_\mathrm{B} = \frac{3\eta V_\mathrm{H}}{k_\mathrm{B} T}. \tag{4}$$

where η is the viscosity of the surrounding liquid and $V_\mathrm{H} = (1 + \delta/R)^3 V_\mathrm{m}$ is the hydrodynamic volume of the magnetic nanoparticle. In the case of the Néel mechanism, the magnetic moment may reverse direction within the particle by overcoming the energy barrier and its relaxation time can be expressed by the relation,

$$\tau_\mathrm{N} = \tau_0 \exp \left(\frac{K V_\mathrm{m}}{k_\mathrm{B} T} \right). \tag{5}$$

where $\tau_0 = 10^{-9}\,\mathrm{s}$ and $K = 23\,\mathrm{kJ} \cdot \mathrm{m}^{-1}$ (for magnetite) is the magnetocrystalline constant. Since Brownian and Néel processes occur in parallel, the effective relaxation time is given by

$$\frac{1}{\tau} = \frac{1}{\tau_\mathrm{B}} + \frac{1}{\tau_\mathrm{N}} \tag{6}$$

The above equations show that the Brownian relaxation time relies on the hydrodynamic particle size. Thus, from a comparison of the experimental results of the initial rate of the temperature rise, $(\Delta T/\Delta t)_{t=0}$, with the predictions of Eq. 3, the thickness of the surfactant layers can be calculated. Figure 8 shows the experimental results of the temperature rise rate against the magnetic field strength together with the theoretical values calculated using Eq. 3 (solid lines). To calculate the rate of temperature rise from the magnetic field power dissipation, the following formula was used:

$$\left(\frac{\Delta T}{\Delta t} \right)_{t=0} = \frac{P}{\rho c_p} \tag{7}$$

where c_p is the heat capacity. The specific heat capacity of a nanoparticle suspension before and after PEG coating was measured using DSC. The dependence of the specific heat on temperature for all samples studied is shown in Fig. 9.

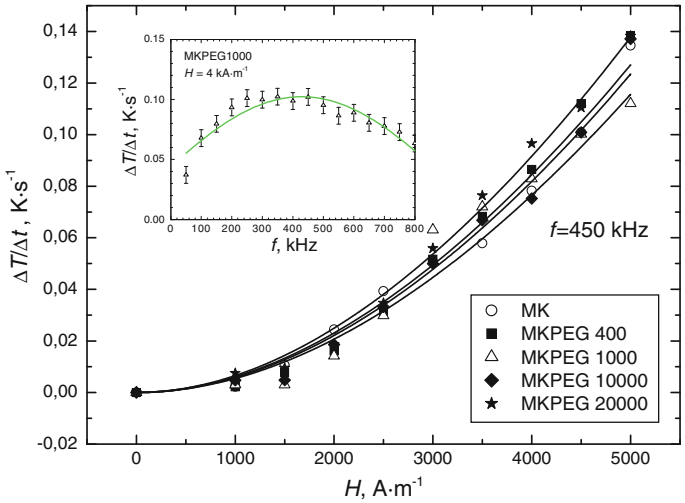

Fig. 8 Temperature rise rate against magnetic field strength (*inset* shows $\Delta T/\Delta t$ as a function of alternating magnetic field frequency). *Solid lines* from down to up correspond to MKPEG10 000, MKPEG1000, MKPEG400, and MKPEG20 000 samples, respectively, and were calculated according to Eq. 3

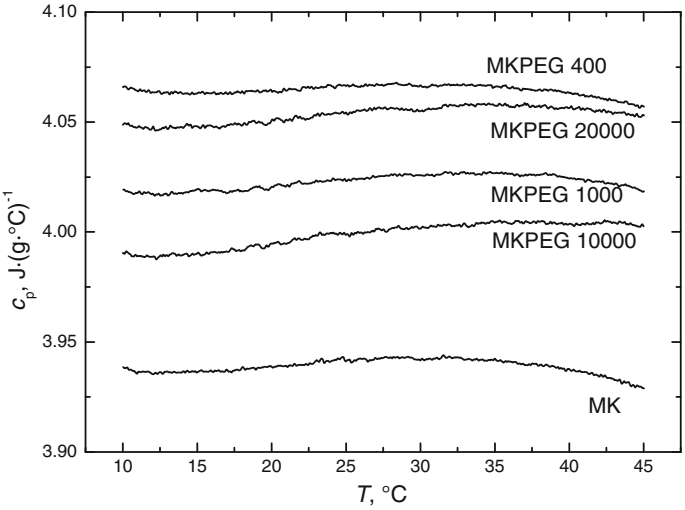

Fig. 9 Heat capacity versus temperature of PEG-stabilized magnetic fluids. *Curves* from down to up correspond to MK, MKPEG10 000, MKPEG1000, MKPEG20 000, and MKPEG400 samples, respectively

For MKPEG400, MKPEG1000, and MKPEG10 000 samples, the best agreement between experimental and theoretical values was obtained for $\delta = 5$ nm as the total thickness of both sodium oleate and PEG layers. For the MKPEG20 000 sample, the best agreement was obtained for $\delta = 3$ nm. Assuming the thickness of sodium oleate layer to be 2 nm, one obtains the value of 3 nm for the thickness of the PEG layer in the case of MKPEG400, MKPEG1000, and PEG10 000 samples and the value of

Table 3 SAR values of PEG-stabilized magnetic nanoparticles calculated from Eq. 8

	MK	MK400	MK1000	MK10 000	MK20 000
C_p ($J \cdot g^{-1} \cdot K^{-1}$)	3.94135	4.06638	4.02313	3.99884	4.05432
ρ ($g \cdot cm^{-3}$)	1.0624	1.0631	1.0641	1.0655	1.063
m_m	0.05656				
SAR ($W \cdot g^{-1}$) (450 kHz, 5 $kA \cdot m^{-1}$)	9.49 ± 0.26	10.47 ± 0.34	9.39 ± 0.46	9.80 ± 0.23	10.66 ± 0.40
SAR ($W \cdot g^{-1}$) (450 kHz, 10 $kA \cdot m^{-1}$) by extrapolation	37.98 ± 1.05	41.89 ± 1.37	37.58 ± 1.83	39.20 ± 0.92	42.62 ± 1.59

1 nm for the thickness of the PEG layer in the case of MKPEG20 000. These findings agree with small angle neutron scattering (SANS) measurements carried out by Feoktystov et al. [19]. According to their evaluation, the thickness of the PEG shell around magnetite nanoparticles was not more than 3 nm. A similar dependence of the thickness of the PEG layer on the molecular weight was observed in the experiment carried out by Zdyrko et al. [20] where the PEG chains of different molecular weights were attached to the silicon substrate via the PGMA primary layer by grafting from the melt at 110 °C. The maximum thickness of the attached film was dependent on the length of the polymer chains being grafted. The higher thickness (8 nm to 11 nm) was achieved for the shorter chains ((2700, 5000, and 10 000) $g \cdot mol^{-1}$). The higher molecular weights ((24 000, 42 000, and 100 000) $g \cdot mol^{-1}$) were grafted at smaller thicknesses (5 nm to 6 nm).

To compare the heating properties of the magnetic fluid samples with different molecular weights of PEG, the specific absorption rate (*SAR*) was calculated. The *SAR* is defined as the amount of heat released by a unit weight of the magnetic material m_m per unit time:

$$SAR = \frac{c_p \rho}{m_m} \left(\frac{\Delta T}{\Delta t} \right)_{t=0} . \tag{8}$$

The values of *SAR* calculated according to Eq. 8 are listed in Table 3. As is seen from the table, the additional biocompatible layer has not been found to exert any influence on the calculated values of *SAR*.

4 Conclusions

The magnetic measurements confirmed the superparamagnetic behavior of the magnetic nanoparticles, and magnetic hysteresis was not observed in the studied samples. The TEM image showed that nanoparticles were nearly spherical in shape and constituted a polydispersed system with a log-normal particle size distribution and a mean magnetic core diameter of about 10 nm. The molecular weight of PEG, which was used as biocompatible coatings, had an effect on the density and rheological properties of water-based magnetic fluids but did not significantly affect the thermal properties of

the studied samples, including their self-heating in the alternate magnetic field. The thickness of the PEG layer calculated from the experimental data of the temperature rise rates as a function of magnetic field strength appeared to be dependent on the PEG molecular weight.

Acknowledgments Work was supported by the Project for Polish–Slovak Bilateral Cooperation No. APVV SK-PL-0069-09/8158/2010. The studies were supported by the Slovak Academy of Sciences VEGA 2/0051/09, Centre of Excellence SAS Nanofluids, Project No. 26220220005 in frame of Structural Funds.

Open Access This article is distributed under the terms of the Creative Commons Attribution Noncommercial License which permits any noncommercial use, distribution, and reproduction in any medium, provided the original author(s) and source are credited.

References

1. D.L. Leslie-Pelecky, V. Labhasetwar, R.H. Kraus, Jr., in *Advanced Magnetic Nanostructures*, ed. by D. Sellmyer, R. Skomski (Springer, New York, 2006), pp. 461–482
2. Y.J. Chen, J. Tao, F. Xiong, J.B. Zhu, N. Gu, K.K. Geng, Pharmazie **65**, 481 (2010)
3. Y. Zhang, N. Kohler, M. Zhang, Biomaterials **23**, 1553 (2002)
4. A.K. Gupta, A.S.G. Curtis, J. Mater. Sci. Mater. Med. **15**, 493 (2004)
5. M.M. Yallapu, S.P. Foy, T.K. Jain, V. Labhasetwar, Pharm. Res. **27**, 2283 (2010)
6. A. Skumiel, A. Józefczak, T. Hornowski, J. Phys. Conf. Ser. **149**, 012111 (2009)
7. A. Józefczak, T. Hornowski, A. Skumiel, M. Łabowski, M. Timko, P. Kopčanský, M. Koneracká, A. Szlaferek, W. Kowalski, J. Magn. Magn. Mater. **321**, 1505 (2009)
8. V. Závišová, M. Koneracká, M. Múčková, J. Lazová, A. Juríková, G. Lancz, N. Tomašovičová, M. Timko, J. Kováč, I. Vávra, M. Fabián, A.V. Feoktystov, V.M. Garamus, M.V. Avdeev, P. Kopčanský, J. Magn. Magn. Mater. **323**, 1408 (2011)
9. M.V. Avdeev, A.V. Feoktystov, P. Kopčanský, G. Lancz, Garamus V.M., R. Willumeit, M. Timko, M. Koneracká, V. Závišová, N. Tomašovičová, A. Juríková, K. Csach, L.A. Bulavin, J. Appl. Cryst. **43**, 959 (2010)
10. M. Rasa, Eur. Phys. J. E **2**, 265 (2000)
11. S. Liufu, H. Xiao, Y. Li, Powder Technol. **145**, 20 (2004)
12. T.J. Daou, L. Li, P. Reiss, V. Josserand, I. Texier, Langmuir **25**, 3040 (2009)
13. J. Ren, H. Hong, T. Ren, X. Teng, React. Funct. Polym. **66**, 944 (2006)
14. C. Groß, K. Büscher, E. Romanus, C.A. Helm, W. Weitschies, Eur. Cell. Mater. **3** (suppl. 2), 163 (2002)
15. X. Qiao, M. Bai, K. Tao, X. Gong, R. Gu, H. Watanabe, K.S.J. Wu, X. Kang, Nihon Reoroji Gakkaishi **38**, 23 (2010)
16. R.Y. Hong, S.Z. Zhang, Y.P. Han, H.Z. Li, J. Ding, Y. Zheng, Powder Technol. **170**, 1 (2006)
17. A. Skumiel, A. Józefczak, M. Timko, P. Kopčanský, F. Herchl, M. Koneracká, N. Tomašovičová, Int. J. Thermophys. **28**, 1461 (2007)
18. R.E. Rosensweig, J. Magn. Mater. **252**, 370 (2002)
19. A.V. Feoktystov, L.A. Bulavin, M.V. Avdeev, V.M. Garamus, P. Kopcansky, M. Timko, M. Koneracka, V. Zavisova, Ukr. J. Phys. **54**, 348 (2009)
20. B. Zdyrko, S.K. Varshney, I. Luzinov, Langmuir **20**, 6727 (2004)